Physical and chemical characterization of combinatorial metal gate electrode Ta–C–N library film

K.-S. Chang,[1,2,a)] M. L. Green,[1] I. Levin,[1] J. R. Hattrick-Simpers,[1] C. Jaye,[1] D. A. Fischer,[1] I. Takeuchi,[2] and S. De Gendt[3]
[1]*National Institute of Standards and Technology (NIST), Gaithersburg, Maryland 20899, USA*
[2]*Department of Materials Science and Engineering, University of Maryland, College Park, Maryland 20742, USA*
[3]*IMEC, Kapeldreef 75, B-3001 Leuven, Belgium and Department of Chemistry, KU Leuven, 3000 Leuven, Belgium*

(Received 19 February 2010; accepted 20 April 2010; published online 13 May 2010)

This paper reports comprehensive structural and chemical analyses for the combinatorial Ta–C–N/HfO_2 system, crucial data for understanding the electrical properties of Ta–C–N/HfO_2. Combinatorial Ta–C–N "library" (composition spread) films were deposited by magnetron sputtering. Electron probe wavelength dispersive spectroscopy and x-ray fluorescence-yield near-edge spectroscopy were used to quantitatively determine the composition across these films. Scanning x-ray microdiffractometry determined that a solid solution of $Ta(C,N)_x$ forms and extends to compositions ($0.3 \leq Ta \leq 0.5$ and $0.57 \leq Ta \leq 0.67$) that were previously unknown. The thermal stability of the Ta–C–N/HfO_2 library was studied using high resolution transmission electron microscopy, which shows Ta–C–N/HfO_2/SiO_2/Si exhibiting good thermal stability up to 950 °C. © *2010 American Institute of Physics*. [doi:10.1063/1.3428788]

The microelectronics industry is exploring replacement materials for the traditional gate stack [SiO_2 gate dielectric and polycrystalline silicon (poly-Si) gate electrode], since aggressive scaling has pushed it to its fundamental materials limit.[1] In the past decade, a huge effort has been made to extensively study high-k gate dielectrics, and HfO_2 has been identified as a promising replacement for SiO_2.[2,3] However, the selection of metal gates compatible with high-k gate dielectrics remains complicated by numerous issues, such as achieving a suitable work function (Φ_m), and high temperature (at least to 1000 °C) thermal stability of the films and interfaces.[4]

The metal gate electrode system Ta–C–N has attracted attention[5–7] due to its tunable Φ_m, high temperature and chemical stability, and good mechanical properties. However, physical and electrical characterization over a wide composition range in a ternary system is too tedious to carry out using the conventional one-composition-at-a-time strategy. Combinatorial methodology, which enables hundreds of different samples to be made and characterized in parallel, is a much more efficient way to approach the problem.[8–10] The goal of this research is to systemically characterize the composition, structure, and interfacial quality of Ta–C–N films libraries on HfO_2/SiO_2/Si.

A radio frequency reactive magnetron sputtering system[11] was employed to deposit the Ta–C–N libraries at room temperature. Ta and C targets were mounted in two separate guns, and reactively sputtered in Ar/N_2 at a pressure of 0.6 Pa. The details of combinatorial library synthesis by sputtering are published elsewhere.[12,13] The library film, deposited on HfO_2, is about 50 nm thick and about 15 $\times 15$ mm^2 in size. Rapid thermal anneals (RTAs) at 950 °C were implemented to determine the thermal stability of the Ta–C–N/HfO_2/SiO_2/Si gate stacks. All library films were subjected to a forming gas anneal (FGA) at 400 °C for 30 min to reduce the interface state densities (D_{it}).

Electron probe wavelength dispersive spectroscopy (WDS) (energy of 15 keV, current of 50 nA, and a probe diameter of 30 μm) was used to determine the variation in the Ta content. An integrated intensity of the L_α line of Ta (7.1 keV), measured across the film, was assumed to reflect the Ta concentration because the corrections for the atomic number, absorption, and fluorescence (i.e., ZAF correction) are small since both C and N are much lighter than Ta. X-ray fluorescence-yield near-edge spectroscopy (FYNES),[14] carried out on the NIST U7A beamline at the National Synchrotron Light Source, enabling not only the identification of chemical bonds but a determination of their relative number densities within a sample, was used to measure the C/N ratio across the library films. A Nylon 6 film, with its known C/N ratio (=6), was used to calibrate the FYNES measurements. In addition, pure films of TaN_x and CN_x were deposited for the purpose of internal calibration/reference. A scanning x-ray microdiffractometer, with a beam diameter of 500 μm, was used to study structure evolution in the Ta–C–N libraries. Cross-sections of samples cut from selected locations in the combinatorial libraries were examined in a high resolution transmission electron microscope (HRTEM), equipped with a postcolumn imaging filter and a charge-coupled device (CCD) camera. Electron energy loss spectra (EELS) were recorded using an imaging filter with the microscope operated in the TEM imaging mode. The interfaces in the Ta–C–N/HfO_2/SiO_2/Si multilayered gate stack structures were oriented parallel to the energy dispersion direction so that the two-dimensional EELS spectra recorded on the CCD camera were spatially resolved across the layer stack. Different portions of the EELS spectra were collected separately to maintain high ($\approx$1 nm) spatial resolution.

Figure 1(a) shows the measured fluorescence yields of C and N for following four samples: a TaN_x film, a CN_x film, a

a)Electronic mail: kao-shuo.chang@nist.gov.

 © 2010 American Institute of Physics

Downloaded 13 May 2010 to 129.6.196.158. Redistribution subject to AIP license or copyright; see http://apl.aip.org/apl/copyright.jsp

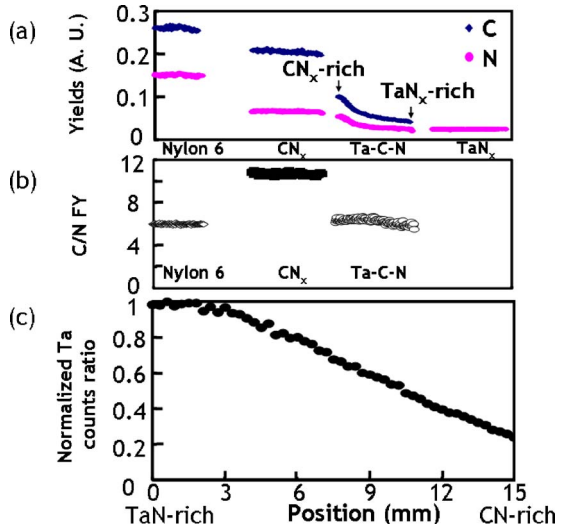

FIG. 1. (Color online) Compositional analysis for the four samples: (a) shows the measured fluorescence yields of C and N from Nylon 6, CN_x, and a Ta–C–N library film, and the fluorescence yields of N from TaN_x, using a FYNES setup; (b) shows the C/N ratios for the samples; (c) shows the Ta ratio, normalizing the maximum intensity to 1, determined by electron probe WDS.

Ta–C–N library sample, and a Nylon 6 film. As seen in the Fig. 1(a), Nylon 6 and CN_x show constant C and N fluorescence yields across their sample areas. Likewise, TaN_x shows constant N fluorescence yield, as expected. A traceable small amount of C has been observed in the TaN_x films, most probably as a result of contamination in the sputtering chamber. A small difference is observed, however, between the N yields of the CN_x and TaN_x samples, most probably due to a difference in their abilities to incorporate N.[15,16]

The Ta–C–N library film, in contrast, yields C and N signals that vary between those of the CN_x and TaN_x films. The N signal decreases from the CN_x-rich end to the TaN_x-rich end, consistent with the N variation for the pure CN_x and TaN_x films. However, the C signal does not vary over a wide range, as it is much lower close to the CN_x-rich end than expected (compared to the CN_x sample), and slightly higher close to the TaN_x-rich end. This can be explained in the following way: (1) the pure CN_x and TaN_x regions are not achievable in the library film because both the Ta and C targets are reactively sputtered continuously, and there is a small gap between the moving shutter[12,13] and the substrate that allows the introduction of a small amount of material from one target when the other target is in the deposition position, and (2) the resulting small amount of TaN_x introduced close to the CN_x-rich end of the library film limits the formation of CN_x, since a solid solution of $Ta(C,N)_x$ is more thermodynamically favorable than CN_x.[17] C competes unfavorably with N for the available octahedral interstitial sites in Ta–C–N during the reactive sputtering process.

Figure 1(b) shows the C/N ratios. The C/N ratio of Nylon 6 was normalized to 6, and then compared to the other samples. The corresponding C/N ratio for pure CN_x is ≈11. The C/N ratio of our Ta–C–N library film did not vary significantly, between ≈6.5 (the CN_x-rich end) to ≈5.5 (the TaN_x-rich end), for the reasons previously discussed. Figure 1(c) shows the Ta variation determined by electron probe WDS for the Ta–C–N library. The intensity of Ta was monitored as a function of position to determine the relative amount of Ta present at each point along the library, and then normalized to 1 for the maximum intensity. A linearly decreasing trend was seen from the TaN_x-rich end toward the CN_x-rich end.

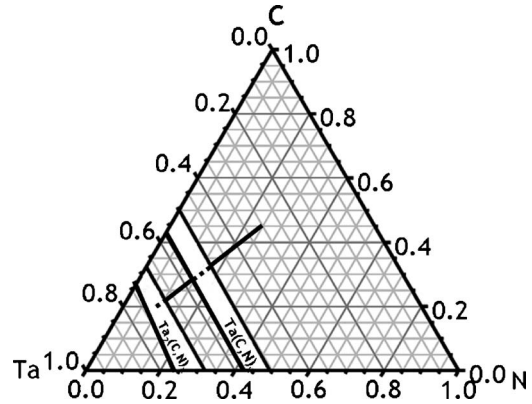

FIG. 2. Ta–C–N library film compositional data plotted in the ternary composition space (the black solid and dashed line). $Ta(C,N)_x$ and $Ta_2(C,N)_x$ equilibrium phase regions are also shown (Ref. 18).

Combining the results from WDS and FYNES-based measurements, the compositional range of the Ta–C–N library film is plotted (the black solid and dashed line) in the ternary phase space in Fig. 2. Here we assume that no other elements (e.g., oxygen) are incorporated into the library. In fact, oxygen has been found in the library film after annealing (to be discussed later). The equilibrium phase fields for $Ta(C,N)_x$ and $Ta_2(C,N)_x$ (Ref. 18) are also plotted in Fig. 2.

Figure 3 shows x-ray diffraction scans as a function of position on the library. The spectra were recorded using the ω-scan mode, and intensities are integrated in the χ direction for each 2θ angle. As seen in Fig. 3(a), a three-dimensional plot of the Ta–C–N library, polycrystalline $Ta(C,N)_x$ is observed. The (111) peak of the $Ta(C,N)_x$ face centered cubic (FCC) phase dominates and the (200) $Ta(C,N)_x$ peak is very weak; thus the film is highly textured. The intensity distribution (peak width) and average 2θ value of the (111) peak continuously changes as a function of position, that is, as a function of composition. To further illustrate this, a top view of the plot is shown in Fig. 3(b). The (111) peak is observed systematically shifting from ≈35.8° (the TaN_x-rich end) to

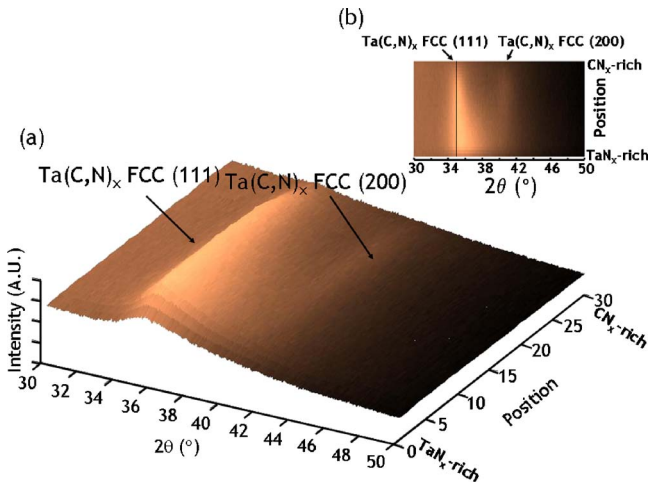

FIG. 3. (Color online) X-ray microdiffraction spectra showing (a) peak intensity as a function of 2θ and film composition (position) and (b) top view of the data in (a).

Downloaded 13 May 2010 to 129.6.196.158. Redistribution subject to AIP license or copyright; see http://apl.aip.org/apl/copyright.jsp

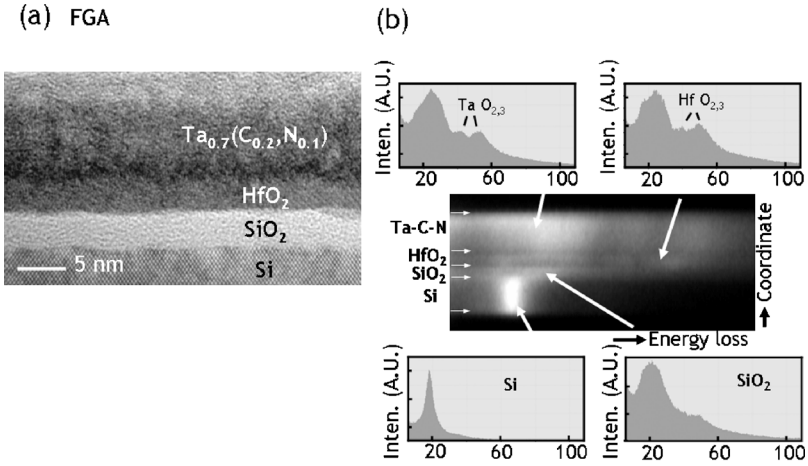

FIG. 4. (Color online) HRTEM images and EELS: (a) HRTEM image of the $Ta_{0.7}(C_{0.2},N_{0.1})/HfO_2$(3 nm)/$SiO_2$(5 nm)/Si multilayer structure, after FGA and (b) EELS spectra line images and the corresponding low loss part of the spectrum for each layer.

≈35.1° (the CN_x-rich end), as a result of more extensive incorporation of C and N into the interstitial sites of $Ta(C,N)_x$, [discussed in Fig. 1(a)]. C atoms, whose radius (≈0.091 nm) is significantly larger than that of N (≈0.075 nm), expand the lattice, and shift the diffraction peak to a lower 2θ value, implying the formation of a solid solution of $Ta(C,N)_x$. Our composition analysis data (Fig. 2) shows significant overlap (the dashed line) with the $Ta(C,N)_x$ phase field, but only a small overlap with the $Ta_2(C,N)_x$ region,[16] consistent with the x-ray diffraction results. In addition, our x-ray diffraction results indicate that the $Ta(C,N)_x$ solid solution phase field in thin films can extend over the compositions (the solid line) that were previously unknown.[16]

Figure 4 shows typical cross section HRTEM images and EELS spectra of the Ta–C–N/HfO_2(3 nm)/SiO_2(5 nm)/Si multilayer structures, for compositions close to the TaN_x-rich end, i.e., ≈$Ta_{0.7}(C_{0.2},N_{0.1})$, after FGA. As seen in Fig. 4(a), after FGA, most of the HfO_2 layer is still amorphous, while the $Ta_{0.7}(C_{0.2},N_{0.1})$ composition exhibits some crystallinity, consistent with the x-ray microdiffraction results. The low loss part of the spectrum is distinct for all the constituent layers and contains well-defined Hf and Ta $O_{2,3}$ core edges [Fig. 4(b)]. EELS spectrum-lines [Fig. 4(b)] exhibit abrupt changes across each interface which indicates lack of significant interlayer reactions. Presence of O in the top part of the Ta–C–N layer was confirmed indicating some surface oxidation upon FGA. After RTA at 950 °C, both the $Ta_{0.7}(C_{0.2},N_{0.1})$ and HfO_2 layers are crystalline. However, the sharp and well-defined interfaces for each layer are preserved suggesting good thermal stability of the multilayer structure after such high temperature exposure (not shown).

In conclusion, we have deposited Ta–C–N library films on HfO_2/SiO_2 by magnetron sputtering, with wide, moderate, and small composition variations in the elements Ta, C, and N, respectively, as evidenced by electron probe WDS and FYNES. X-ray microdiffractometry suggests the formation of a solid solution of $Ta(C,N)_x$, which spans composition ranges ($0.3 \leq Ta \leq 0.5$ and $0.57 \leq Ta \leq 0.67$) much broader than previously reported. The interfacial stability as a function of annealing temperature at the Ta–C–N/HfO_2 and HfO_2/SiO_2 interfaces was studied using HRTEM, which shows the Ta–C–N/HfO_2/SiO_2/Si structure exhibiting good thermal stability up to 950 °C. The structural and chemical analyses of the combinatorial Ta–C–N/HfO_2 system presented in this study provide crucial supporting data for understanding the electrical properties of gate stacks using Ta–C–N metal gate electrodes.

[1]International Technology Roadmap for Semiconductors 2007, http://public.itrs.net.
[2]G. D. Wilk, R. M. Wallace, and J. M. Anthony, J. Appl. Phys. **89**, 5243 (2001).
[3]G. Bersuker, P. Zeitzoff, G. Brown, and H. R. Huff, Mater. Today **7**, 26 (2004).
[4]G. A. Brown, P. M. Zeitzoff, G. Bersuker, and H. R. Huff, Mater. Today **7**, 20 (2004).
[5]J. K. Schaeffer, C. Capasso, R. Gregory, D. Gilmer, L. R. C. Fonseca, M. Raymond, C. Happ, M. Kottke, S. B. Samavedam, P. J. Tobin, and B. E. White, Jr., J. Appl. Phys. **101**, 014503 (2007).
[6]S. M. Aouadi, Y. Zhang, P. Basnyat, S. Stadler, P. Filip, M. Williams, J. N. Hilfiker, N. Singh, and J. A. Woollam, J. Phys.: Condens. Matter **18**, 1977 (2006).
[7]T. J. Park, J. H. Kim, J. H. Jang, K. D. Na, C. S. Hwang, G.-M. Kim, K. J. Choi, and J. H. Jeong, Appl. Phys. Lett. **92**, 202902 (2008).
[8]X.-D. Xiang and P. G. Schultz, Physica C **282**, 428 (1997).
[9]X.-D. Xiang, X. Sun, G. Briceno, Y. Lou, K.-A. Wang, H. Chang, W. G. Wallace-Freedman, S.-W. Chen, and P. G. Schultz, Science **268**, 1738 (1995).
[10]K.-S. Chang, M. Green, J. Suehle, E. Vogel, H. Xiong, J. Hattric-Simpers, I. Takeuchi, O. Famodu, K. Ohmori, P. Ahmet, T. Chikyow, P. Majhi, B.-H. Lee, and M. Gardner, Appl. Phys. Lett. **89**, 142108 (2006).
[11]Certain commercial equipment, instruments, or materials are identified in this document. Such identification does not imply recommendation or endorsement by the National Institute of Standards and Technology, nor does it imply that the products identified are necessarily the best available for the purpose.
[12]K.-S. Chang, M. L. Green, J. R. Hattrick-Simpers, I. Takeuchi, J. S. Suehle, O. Celik, and S. De Gendt, IEEE Trans. Electron Devices **55**, 2641 (2008).
[13]M. L. Green, K.-S. Chang, S. De Gendt, T. Schram, and J. Hattrick-Simpers, Microelectron. Eng. **84**, 2209 (2007).
[14]T. Hemraj-Benny, S. Banerjee, S. Sambasivan, M. Balasubramanian, D. Fischer, D. Lowndes, W. Han, J. Misewich, and S. Wong, Small **2**, 26 (2006).
[15]H. B. Nie, S. Y. Xu, S. J. Wang, L. P. You, Z. Yang, C. K. Ong, J. Li, and T. Y. F. Liew, Appl. Phys. A: Mater. Sci. Process. **73**, 229 (2001).
[16]D. M. Teter and R. J. Hemley, Science **271**, 53 (1996).
[17]D. R. Gaskell, *Introduction to the Thermodynamics of Materials* (Taylor & Francis, London, 2003).
[18]K. Frisk, J. Alloys Compd. **278**, 216 (1998).

Downloaded 13 May 2010 to 129.6.196.158. Redistribution subject to AIP license or copyright; see http://apl.aip.org/apl/copyright.jsp